**S. Orphanoudakis, P. Trahanias, J. Crowley, N. Katevas (Eds.),**
**Proc. Computer Vision and Mobile Robotics Workshop**
**(CVMR '98, Santorini, Sept. 17–18, 1998), pp. 115–122, 1998**

# On Discontinuity-Preserving Optic Flow

**Joachim Weickert***

DIKU, Universitetsparken 1
2100 Copenhagen, Denmark

**Abstract.** We investigate a modification of Horn and Schunck's approach which leads to a better preservation of flow discontinuities. It replaces the quadratic smoothness term by a nonquadratic one. Energy minimization by steepest descent leads to a system of two nonlinear diffusion–reaction equations with a single common nonlinear diffusivity. This enables us to make use from techniques for nonlinear diffusion filtering of colour images. A recently discovered nonlinear diffusion algorithm is extended to the efficient approximation of the optic flow equations. Experiments on sequences of real-images illustrate that the presented approach leads to more realistic optic flow estimates than the Horn and Schunck method.

**Key Words:** Optic flow, regularization, nonlinear diffusion, vector-valued images, additive operator splitting.

**CR Subject Classification:** I.4.8, I.4.3, G.1.8.

## 1 Introduction

The recovery of motion is necessary for many artificial vision systems, since it can be used for instance to obtain information about depth and egomotion, and it may help to segment a scene into semantically correct regions. Efficient and reliable motion estimation is therefore of central importance for fields such as vision-based robot navigation. Motion is linked to the notion of optic flow, the distribution of apparent velocities of movement of brightness pattern in an image.

The pioneering work of Horn and Schunck [9] has triggered a vast amount of research on the determination of optic flow. An overview of the most important algorithms and an evaluation of their performance can be found in [1].

The determination of optic flow is a classic ill-posed problem in computer vision [2], and it requires to be supplemented with additional regularizing assumptions. The regularization by Horn and Schunck assumes that the optic flow field is smooth. However, since many natural image sequences are better described in terms of piecewise smooth flow fields with discontinuities in between, much research has been done to modify the Horn and Schunck approach in order to permit such discontinuous flow fields; see [4, 6, 10, 11, 12, 15, 18] and the references therein.

The work to be presented here is in line with this research. We investigate a modification of Horn and Schunck's energy functional which replaces the quadratic smoothness constraint by a novel nonquadratic one. Energy minimization is performed by applying gradient descent. This leads to a stongly coupled system of two nonlinear diffusion–reaction equation with a common diffusivity as in nonlinear vector–valued diffusion filtering. An efficient numerical approximation is applied which results from an extension of a recently developed additive operator splitting (AOS) technique [21] to the optic flow equations. Each iteration requires

* E-mail: joachim@diku.dk

only the solution of simple tridiagonal linear systems of equations which can be performed in linear complexity using a modified Gaussian algorithm.

The paper is organized as follows. In Section 2 we review Horn and Schunck's optic flow approach, and Section 3 describes our modification. The basic ideas behind the numerical approximation are described in Section 4, and Section 5 illustrates the potential of our approach by appying it to natural test images. The paper is concluded with a summary in Section 6.

**Related work.** Isaac Cohen [4] pioneered the field of investigating nonquadratic smoothness constraints for optic flow calculations. His $L^1$ minimization is related to total variation denoising strategies as introduced by Rudin *et al.* [16]. A method identical to Cohen's approach has been studied later on by Kumar *et al.* [10]. Deriche *et al.* [6] propose to use another nonquadratic smoothness term which relates optic flow computations to nonlinear diffusion filtering. Whereas early nonlinear diffusion approaches such as [14, 13] use diffusivities which may create ill-posed filters, the approach by Deriche *et al.* leads to the diffusivities of Charbonnier *et al.* [3]. They correspond to monotone flux functions for which one can guarantee well-posedness of the process and convergence of standard approximations [17]. We replace the smoothness term of Deriche *et al.* by a term which leads to a stronger coupling between the resulting partial differential equations for the optic flow components: it uses a common diffusivity for both components ensuring that discontinuities appear at the same locations. This coupling also appears in nonlinear diffusion filters for vector-valued images as pioneered by Gerig *et al.* [8]. Schnörr [18] designed a related variational technique and used it for postprocessing optic flow calculations. This distinguishes his approach from ours which integrate the regularization already in the energy functional for determining optic flow. The method presented here is also conceptually simpler than the one by Proesmans *et al.* [15] which uses a system of six coupled nonlinear diffusion–reaction equations.

## 2 The Approach of Horn and Schunck

Let us denote an image sequence by some function $f(x, y, t)$ where (x,y) denotes the location within some rectangular image domain $\Omega$ and $t$ is the time. The approach of Horn and Schunck [9] attemps to determine the optic flow vector $\mathbf{w} = (u, v)^T$ based on two assumptions:

- Corresponding features are supposed to maintain their intensity over time. This leads to the *optic flow constraint (OFC) equation*
$$f_x u + f_y v + f_t = 0, \tag{1}$$
where the subscripts denote partial derivatives.
Evidently such a single equation is not sufficient to determine the two unknown functions $u$ and $v$ uniquely. When used alone, it only allows to recover the flow component parallel to $\nabla f$. This so-called *normal flow* $w_n$ is given by
$$w_n = -\frac{f_t}{|\nabla f|}. \tag{2}$$
We may add arbitrary tangential components, and the optic flow constraint is still satisfied. This ambiguity is called *aperture problem* and illustrates the ill-posedness of optic flow determination when formulated in terms of the OFC. In order to recover a unique flow field, we need an additional regularizing assumption.
- The regularization by Horn and Schunck consists in assuming that the flow field varies smoothly in space. This can be expressed by requiring that the integral
$$\int_\Omega \left(|\nabla u|^2 + |\nabla v|^2\right) \, dx \, dy \tag{3}$$
should be close to 0. This assumption is called *smoothness constraint.*

In order to satisfy both the optic flow and smoothness constaint as good as possible, they are assembled into an energy functional to be minimized:
$$E(u, v) := \int_\Omega \left(\alpha(f_x u + f_y v + f_t)^2 + (|\nabla u|^2 + |\nabla v|^2)\right) \, dx \, dy \tag{4}$$

where $\alpha > 0$ is the weight of the first summand (data term) relative to the second one (smoothness term).

It is a classic result from the calculus of variations [5, 7] that a solution $(u, v)$ minimizing an energy functional of type

$$E(u,v) := \int_\Omega F(x, y, u, v, u_x, u_y, v_x, v_y)\, dx\, dy \tag{5}$$

satisfies necessarily the so-called Euler equations

$$\partial_x F_{u_x} + \partial_y F_{u_y} - F_u = 0, \tag{6}$$
$$\partial_x F_{v_x} + \partial_y F_{v_y} - F_v = 0 \tag{7}$$

with reflecting boundary conditions:

$$\partial_n u = 0 \quad \text{on } \partial\Omega, \tag{8}$$
$$\partial_n v = 0 \quad \text{on } \partial\Omega. \tag{9}$$

Hereby, $\partial\Omega$ denotes the boundary of the image domain, and $n$ is a normal vector to it.

Applying this relation it is easily seen that minimization of (4) corresponds to solving

$$\Delta u - 2\alpha f_x (f_x u + f_y v + f_t) = 0, \tag{10}$$
$$\Delta v - 2\alpha f_y (f_x u + f_y v + f_t) = 0. \tag{11}$$

These equations can be thought of as the steady-state of the diffusion–reaction processes

$$u_\theta = \Delta u - 2\alpha f_x (f_x u + f_y v + f_t), \tag{12}$$
$$v_\theta = \Delta v - 2\alpha f_y (f_x u + f_y v + f_t). \tag{13}$$

$\Delta$ denotes the Laplace operator, and the parameter $\theta$ is an artificial evolution parameter which should not be mixed up with the time $t$ of the image sequence $f(x, y, t)$. We may also regard (12)–(13) as a gradient descent method for minimizing (4).

We see that the underlying diffusion process to the Horn and Schunck approach is the linear diffusion equation

$$u_\theta = \Delta u. \tag{14}$$

This equation is well-known for its regularizing properties and has been extensively used in the context of Gaussian scale-space; see e.g. [19]. It smoothes, however, also across discontinuities and blurs them. This is the reason why the Horn and Schunck approach creates rather blurry optic flow fields.

## 3 A Modified Smoothness Constraint

The linear diffusion terms $\Delta u$ and $\Delta v$ in (12) and (13), respectively, are caused by the smoothness term in the energy functional (4). It has the structure $T(\sqrt{|\nabla u|^2 + |\nabla v|^2})$, where T is a quadratic function:

$$T(s) = s^2 \tag{15}$$

In order to permit flow fields which preserve discontinuities in a better way, we replace the quadratic smoothness term by the nonquadratic (but still convex) expression

$$T(s) = \lambda^2 \sqrt{1 + s^2/\lambda^2} \qquad (\lambda > 0). \tag{16}$$

The gradient descent equations to the modified energy functional are then given by

$$u_\theta = \operatorname{div}\left(g\left(|\nabla u|^2 + |\nabla v|^2\right) \nabla u\right) - 2\alpha f_x (f_x u + f_y v + f_t), \tag{17}$$
$$v_\theta = \operatorname{div}\left(g\left(|\nabla u|^2 + |\nabla v|^2\right) \nabla v\right) - 2\alpha f_y (f_x u + f_y v + f_t) \tag{18}$$

with a diffusivity function

$$g(s^2) = \frac{1}{\sqrt{1 + s^2/\lambda^2}}. \tag{19}$$

We observe that the diffusivity $g(|\nabla u|^2 + |\nabla v|^2)$, which controls the activity of both diffusion processes, becomes small for large flow gradients. This penalizes diffusion across flow discontinuities and, consequently, help to preserve them in a better way.

Processes of type (17)–(18) are closely related nonlinear diffusion filters for vector-valued images: indeed, for $\alpha \to 0$, these equations become a nonlinear diffusion process for the two-channel image $(u, v)^T$ similar to the one studied by Gerig *et al.* [8]. The latter approach, however, uses diffusivities which may create ill-posed processes. This cannot happen in our case, since convex smoothness terms $T(s)$ in the energy functional create well-posed diffusion–reaction processes [17, 18].

It should also be noted that our approach differs from related ones such as [4, 6, 10] by the fact that it uses a common diffusivity $g(|\nabla u|^2 + |\nabla v|^2)$ for both equations. This has the following favourable consequences:

- The formation of discontinuities is better synchronized between the $u$ and $v$ component than in approaches using $g(|\nabla u|^2)$ for the first and $g(|\nabla v|^2)$ for the second equation.
- The method is rotationally invariant, since the smoothness term $T(\sqrt{|\nabla u|^2 + |\nabla v|^2})$ is invariant under rotations. This is in general no longer true, if $T$ is nonquadratic and expressions of type $T(|\nabla u|)+T(|\nabla v|)$ are used instead of $T(\sqrt{|\nabla u|^2 + |\nabla v|^2})$.

## 4 Numerical Aspects

We approximate the diffusion–reaction system (17)–(18) by finite differences. Derivatives in $x$, $y$ and $t$ are approximated by central differences. The discretization in $\theta$ direction approximates the nonlinear diffusivity at the old level, and the rest of the divergence expression at the new level. Such a semi-implicit approach allows to use large time steps, but requires to solve a linear system of equations in each step. We approximate this linear system by using an additive operator splitting [21]. It leads to tridiagonal systems of equations which can be solved efficiently in linear complexity by a modified Gauß algorithm, the so-called Thomas algorithm. This may be regarded as a separable algorithm using causal and anticausal recursive filters. Schemes of this type are well-suited for parallel architectures [22], and their computational and storage complexity is linear in the pixel number. This makes their use attractive in the context of time-critical applications such as vision-based robot navigation.

Each iteration step proceeds as follows. Let $\tau$ be the step size in $\theta$ direction and let the vectors $\mathbf{f}_x$, $\mathbf{f}_y$ and $\mathbf{f}_t$ denote central difference approximations of $f_x$, $f_y$ and $f_t$ respectively. The vector components describe the results at different pixels. Let the flow components for the first iteration be initialized by the normal flow. The $(k+1)$-th iteration calculates the flow components $\mathbf{u}^{(k+1)}$ and $\mathbf{v}^{(k+1)}$ from $\mathbf{u}^{(k)}$ and $\mathbf{v}^{(k)}$ via

$$\mathbf{u}^{(k+1)} = \frac{1}{2} \sum_{l=1}^{2} \left( \left(1 + 2\alpha\tau \mathbf{f}_x^2\right) I - 2\tau A_l^{(k)} \right)^{-1} \left( \mathbf{u}^{(k)} - 2\alpha\tau \mathbf{f_x} \left( \mathbf{f}_y \mathbf{v}^{(k)} + \mathbf{f}_t \right) \right) \tag{20}$$

$$\mathbf{v}^{(k+1)} = \frac{1}{2} \sum_{l=1}^{2} \left( \left(1 + 2\alpha\tau \mathbf{f}_y^2\right) I - 2\tau A_l^{(k)} \right)^{-1} \left( \mathbf{v}^{(k)} - 2\alpha\tau \mathbf{f_y} \left( \mathbf{f}_x \mathbf{u}^{(k)} + \mathbf{f}_t \right) \right) \tag{21}$$

where the product of two vectors should be understood componentwise, $I$ is the unit matrix, and the matrices $A_1$ and $A_2$ are standard finite difference approximations to the following terms:

$$A_1\mathbf{u} \quad \text{approximates} \quad \partial_x \left( g(|\nabla u|^2 + |\nabla v|^2)\, u_x \right), \tag{22}$$

$$A_2\mathbf{u} \quad \text{approximates} \quad \partial_y \left( g(|\nabla u|^2 + |\nabla v|^2)\, u_y \right). \tag{23}$$

The matrix inversions are realized solving tridiagonal linear systems.

For an extensive discussion on additive operator splitting, the reader is referred to [21]. This class of fast algorithms satisfies recently discovered criteria which ensure reliable discrete nonlinear diffusion filtering [20].

## 5 Experiments

In this section we illustrate the behaviour of our method by applying it to three real-image sequences. The first and second are available via anonymous ftp from `ftp://csd.uwo.ca` under the directory `pub/vision`.

Figure 1 shows Richard Szeliski's Rotating Rubik's Cube sequence. The optic flow between frame 10 and 11 is calculated both for the Horn and Schunck approach and the nonquadratic smoothness term. We observe that the proposed method suffers much less from blurring effects than the Horn and Schunck approach. It is not difficult to recognize the cube from the flow magnitude in Figure 1(e).

Qualitatively similar results can be observed for the Hamburg Taxi Sequence in Figure 2. In particular, the optic flow magnitude depicted in Figure 2(e) allows a rather realistic segmentation of the taxi.

Figure 3 analyses a sequence of a man walking along a hallway. In this example the flow magnitude is thresholded at a value which gives the visually most realistic flow field. The nonquadratic approach appears to give better results again. In contrast to the Horn and Schunck result, most people would have no difficulties to recognize that Figure 3(e) analyses a person.

## 6 Conclusions

We have presented a method for optic flow determination which combines Horn and Schunck's optic flow constraint with a nonquadratic smoothness contraint. The latter one allows to relate this approach to nonlinear diffusion filtering of colour images. Experiments indicate that our method appears favourable over the Horn and Schunck approach for tasks such as motion segmentation.

Future work will be devoted to the exploration of further relations between optic flow determination and nonlinear diffusion filtering as well as to further research on efficient algorithms. It is also planned to make a critical performance analysis using synthetic test sequences for which a ground truth is available and which allows to juxtapose this technique to the established ones which are analysed in [1].

**Acknowledgements.** This work has been done within the EU-TMR network VIRGO. I thank Ole Fogh Olsen and Mads Nielsen for providing the hallway sequence, and Jon Sporring for helping to create the vector plots.

## References

1. J.L. Barron, D.J. Fleet, S.S. Beauchemin, *Performance of optical flow techniques*, Int. J. Comput. Vision, Vol. 12, 43–77, 1994.
2. M. Bertero, T.A. Poggio, V. Torre, *Ill-posed problems in early vision*, Proc. IEEE, Vol. 76, 869–889, 1988.
3. P. Charbonnier, L. Blanc–Féraud, G. Aubert, M. Barlaud, *Two deterministic half-quadratic regularization algorithms for computed imaging*, Proc. IEEE Int. Conf. Image Processing (ICIP–94, Austin, Nov. 13–16, 1994), Vol. 2, IEEE Computer Society Press, Los Alamitos, 168–172, 1994.
4. I. Cohen, *Nonlinear variational method for optical flow computation*, Proc. Eighth Scandinavian Conf. on Image Analysis (SCIA '93, Tromsø, May 25–28, 1993), Vol. 1, 523–530, 1993.
5. R. Courant, D. Hilbert, *Methods of mathematical physics*, Vol. 1, Interscience, New York, 1953.
6. R. Deriche, P. Kornprobst, G. Aubert, *Optical-flow estimation while preserving its discontinuities: A variational approach*, Proc. Second Asian Conf. Computer Vision (ACCV '95, Singapore, December 5–8, 1995), Vol. 2, 290–295, 1995.
7. L.E. Elsgolc, *Calculus of variations*, Pergamon, Oxford, 1961.
8. G. Gerig, O. Kübler, R. Kikinis, F.A. Jolesz, *Nonlinear anisotropic filtering of MRI data*, IEEE Trans. Medical Imaging, Vol. 11, 221–232, 1992.
9. B. Horn, B. Schunck, *Determining optical flow*, Artif. Intell., Vol. 17, 185–203, 1981.
10. A. Kumar, A.R. Tannenbaum, G.J. Balas, *Optic flow: a curve evolution approach*, IEEE Trans. Image Proc., Vol. 5, 598–610, 1996.
11. H.H. Nagel, W. Enkelmann, *An investigation of smoothness constraints for the estimation of displacement vector fields from images sequences*, IEEE Trans. Pattern Anal. Mach. Intell., Vol. 8, 565–593, 1986.
12. P. Nesi, *Variational approach to optical flow estimation managing discontinuities*, Image Vision Comput., Vol. 11, 419–439, 1993.
13. N. Nordström, *Biased anisotropic diffusion - a unified regularization and diffusion approach to edge detection*, Image Vision Comput., Vol. 8, 318–327, 1990.
14. P. Perona, J. Malik, *Scale space and edge detection using anisotropic diffusion*, IEEE Trans. Pattern Anal. Mach. Intell., Vol. 12, 629–639, 1990.
15. M. Proesmans, L. Van Gool, E. Pauwels, A. Oosterlinck, *Determination of optical flow and its discontinuities using non-linear diffusion*, J.-O. Eklundh (Ed.), Computer vision – ECCV '94, Lecture Notes in Computer Science, Vol. 801, Springer, Berlin, 295–304, 1994.

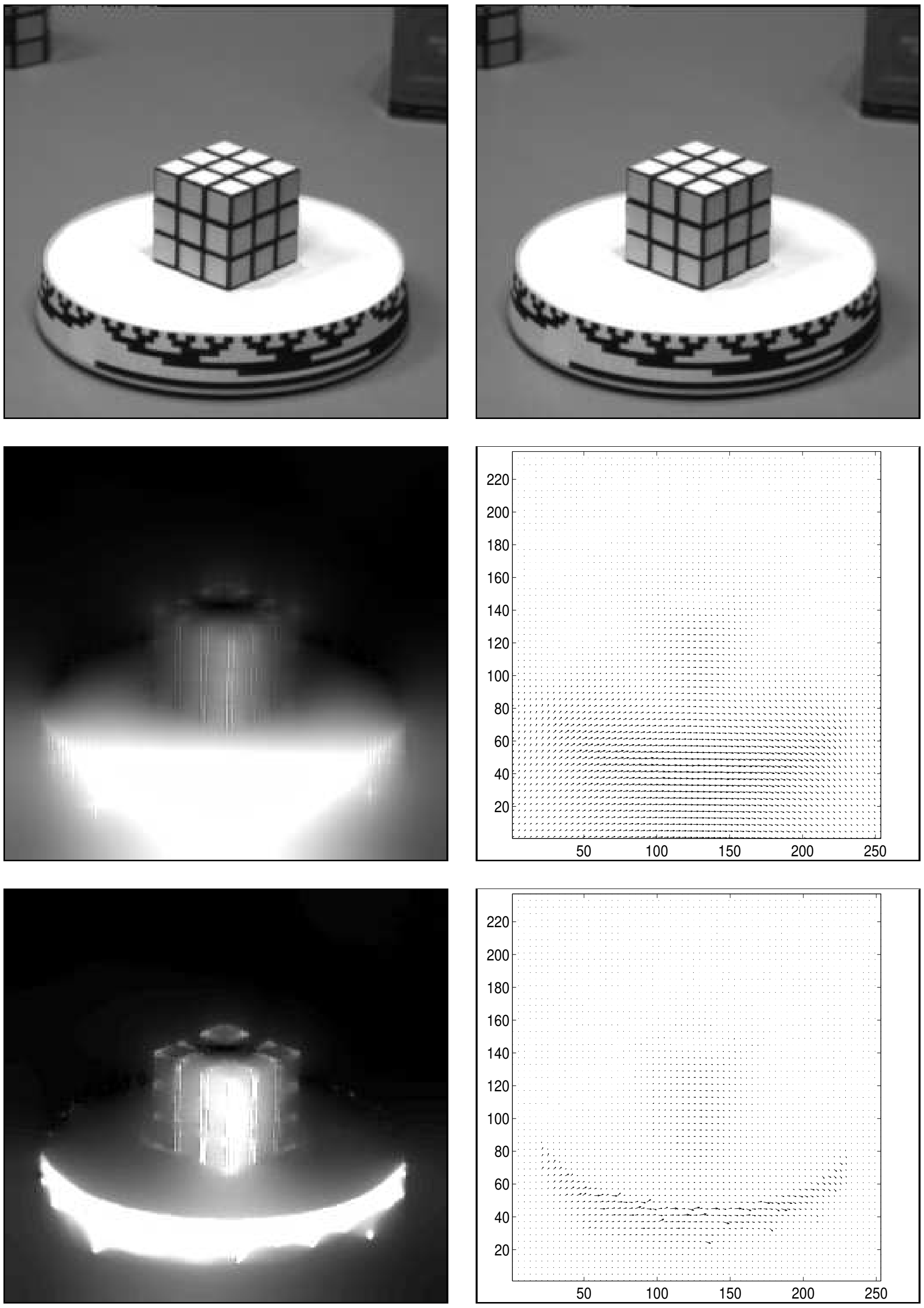


Fig. 1.: Rubik's cube. (A) TOP LEFT: Frame 10. (B) TOP RIGHT: Frame 11. (C) MIDDLE LEFT: Horn and Schunck, optic flow magnitude, $\alpha = 0.0001$. Depicted grey-value range is $[0, 1.05]$. (D) MIDDLE RIGHT: Horn and Schunck, vector plot. (E) BOTTOM LEFT: Nonquadratic smoothness term, optic flow magnitude, $\alpha = 0.0001$, $\lambda = 0.005$. Depicted grey-value range is $[0, 0.52]$. (F) BOTTOM RIGHT: Nonquadratic smoothness term, vector plot.

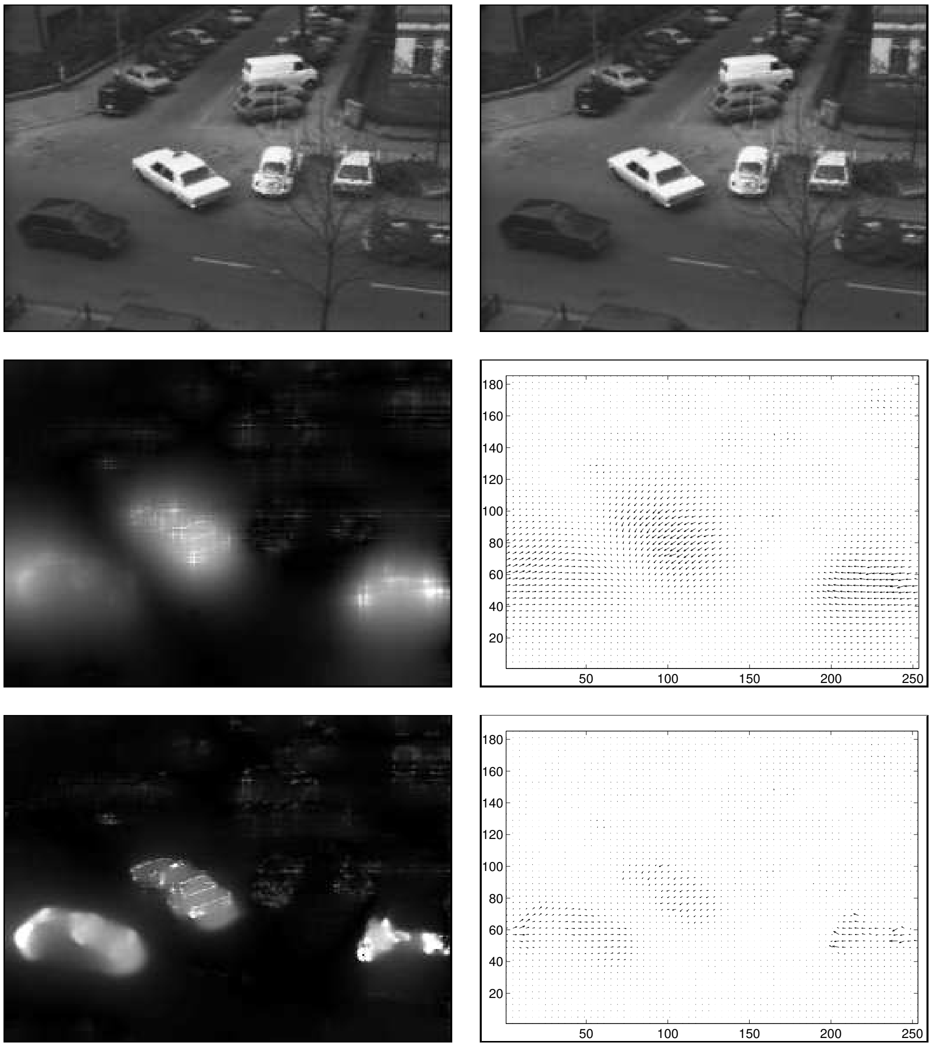


Fig. 2.: Taxi scene. (A) TOP LEFT: Frame 10. (B) TOP RIGHT: Frame 11. (C) MIDDLE LEFT: Horn and Schunck, optic flow magnitude, $\alpha = 0.0001$. Depicted grey-value range is $[0, 1.31]$. (D) MIDDLE RIGHT: Horn and Schunck, vector plot. (E) BOTTOM LEFT: Nonquadratic smoothness term, optic flow magnitude, $\alpha = 0.0001, \lambda = 0.01$. Depicted grey-value range is $[0, 1.62]$. (F) BOTTOM RIGHT: Nonquadratic smoothness term, vector plot.

16. L.I. Rudin, S. Osher, E. Fatemi, *Nonlinear total variation based noise removal algorithms*, Physica D, Vol. 60, 259–268, 1992.
17. C. Schnörr, *Unique reconstruction of piecewise smooth images by minimizing strictly convex non-quadratic functionals*, J. Math. Imag. Vision, Vol. 4, 189–198, 1994.
18. C. Schnörr, *Convex variational segmentation of multi-channel images*, M.-O. Berger, R. Deriche, I. Herlin, J. Jaffré, J.-M. Morel (Eds.), ICAOS '96: Images, wavelets and PDEs, Lecture Notes in Control and Information Sciences, Vol. 219, Springer, London, 201–207, 1996.
19. J. Sporring, M. Nielsen, L. Florack, P. Johansen (Eds.), *Gaussian scale-space theory*, Kluwer, Dordrecht, 1997.
20. J. Weickert, *Anisotropic diffusion in image processing*, Teubner-Verlag, Stuttgart, 1998.
21. J. Weickert, B.M. ter Haar Romeny, M.A. Viergever, *Efficient and reliable schemes for nonlinear diffusion filtering*, IEEE Trans. Image Proc., Vol. 7, 398–410, 1998.
22. J. Weickert, K.J. Zuiderveld, B.M. ter Haar Romeny, W.J. Niessen, *Parallel implementations of AOS schemes: A fast way of nonlinear diffusion filtering*, Proc. 1997 IEEE International Conference on Image Processing (ICIP–97, Santa Barbara, Oct. 26–29, 1997), Vol 3., 396–399, 1997.

This article was processed using the TEX macro package with SIRS98 style

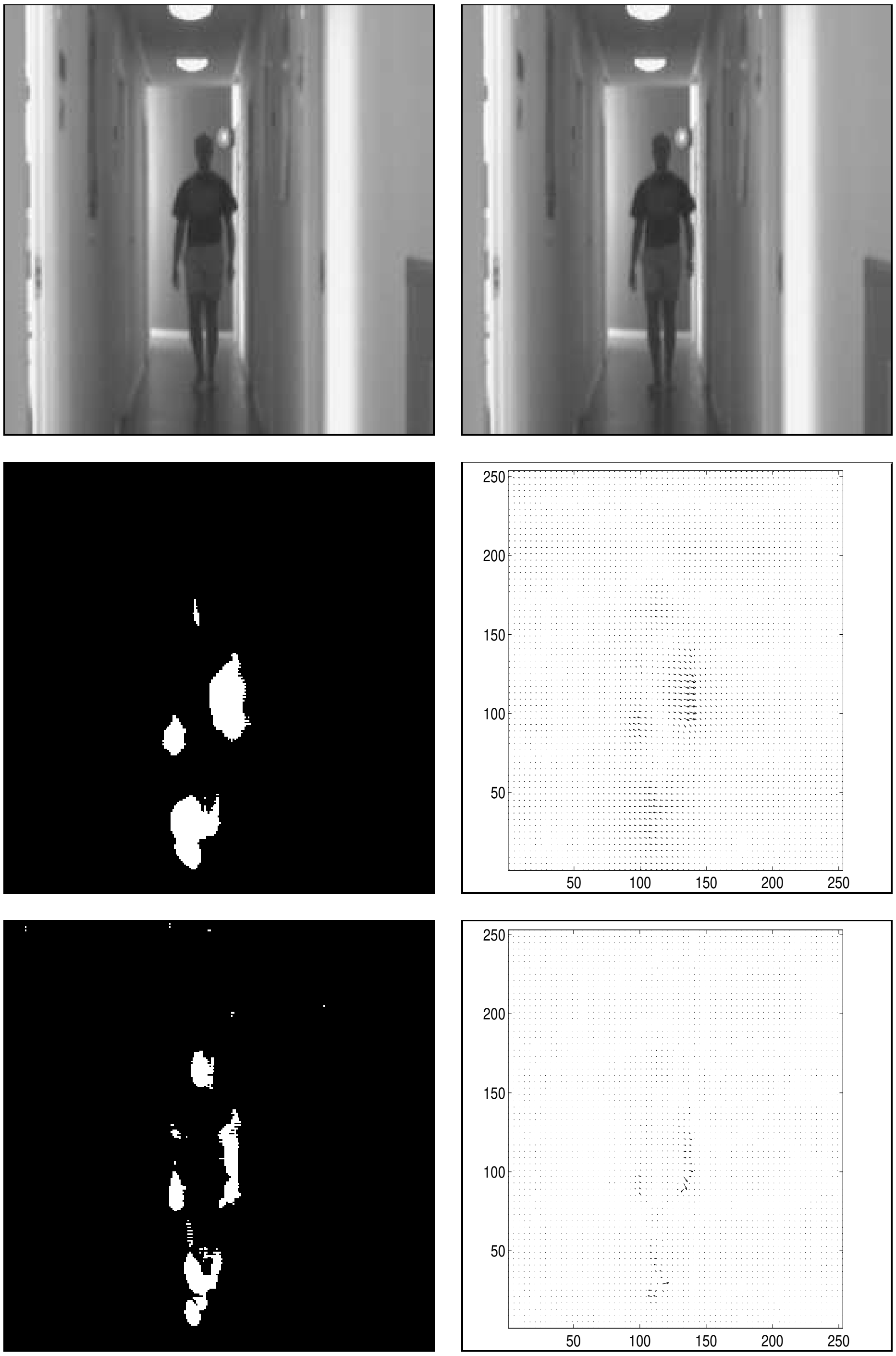


Fig. 3.: Hallway scene. (A) Top Left: Frame 31. (B) Top Right: Frame 32. (C) Middle Left: Horn and Schunck, optic flow magnitude, $\alpha = 0.0001$. Thresholded at 0.19. (D) Middle Right: Horn and Schunck, vector plot. (E) Bottom Left: Nonquadratic smoothness term, optic flow magnitude, $\alpha = 0.0001$, $\lambda = 0.01$. Thresholded at 0.17. (F) Bottom Right: Nonquadratic smoothness term, vector plot.